The Astronomical Journal, 132:1221–1233, 2006 September

CALIBRATION OF SYNTHETIC PHOTOMETRY USING DA WHITE DWARFS

J. B. Holberg[1] and Pierre Bergeron[2]

Received 2006 January 5; accepted 2006 May 9

ABSTRACT

We have calibrated four major ground-based photometric systems with respect to the *Hubble Space Telescope* (*HST*) absolute flux scale, which is defined by Vega and four fundamental DA white dwarfs. These photometric systems include the Johnson-Kron-Cousins *UBVRI*, the Strömgren *uvby* filters, the Two Micron All Sky Survey JHK_s, and the Sloan Digital Sky Survey *ugriz* filters. Synthetic magnitudes are calculated from model white dwarf spectra folded through the published filter response functions; these magnitudes in turn are absolutely calibrated with respect to the *HST* flux scale. Effective zero-magnitude fluxes and zero-point offsets of each system are determined. In order to verify the external observational consistency, as well as to demonstrate the applicability of these definitions, the synthetic magnitudes are compared with the respective observed magnitudes of larger sets of DA white dwarfs that have well-determined effective temperatures and surface gravities and span a wide range in both of these parameters.

Key words: standards — stars: fundamental parameters — stars: individual (Vega) — techniques: photometric — white dwarfs

Online material: machine-readable tables

1. INTRODUCTION

Absolute astrophysical fluxes are important in a number of circumstances. In stellar astronomy, absolute fluxes represent a fundamental link between the predicted fluxes of model stellar atmospheres and the distances and radii of stars. These fluxes are also the basis for establishing such primary quantitative relations as that of the solar luminosity to observed stellar luminosities. The growth of the importance of space-based observations in the IR, UV, far-UV, extreme-UV (EUV), and other bands well outside the optical provides another important application for absolute stellar fluxes. The photometric calibration of these wavelength ranges and the need to unambiguously relate observations in one band to other nonoverlapping bands on the same physical scale depends directly on accurate absolute fluxes. The most important and widely used realization of this objective is now the *Hubble Space Telescope* (*HST*) flux scale, established by R. Bohlin and collaborators. This scale, which formally extends from 1200 Å in the UV to 8000 Å in the red, is discussed below in more detail. Finally, it has recently become evident that efforts to probe the properties of the cosmological dark energy and the evolution of the universe through observations of distant Type Ia supernovae will ultimately require the establishment of very accurate absolute and relative photometric scales that extend well into the near-IR and whose linearity is securely established at magnitudes much fainter than those in common use today.

Stellar photometric systems are generally defined in terms of various combinations of detector and filter response functions, together with observations of sets of standard stars. Intercomparisons of the observed magnitudes and colors in one photometric system with those of another are traditionally made by observing a number of stars in both systems and specified by empirical color-dependent transformation equations. The photometric zero points, or the equivalent monochromatic absolute fluxes in particular passbands, are usually indirectly related back to the fundamental stellar standard star, Vega. For example, the zero point of the Johnson V band is often quoted as the monochromatic flux of Vega at some wavelength near the centroid of the V passband. One frequently used definition of such a flux normalization is that of a hypothetical $V = 0$ mag, Vega-like A0 V star at the top of the Earth's atmosphere with a monochromatic flux at 5500 Å of 3.66×10^{-9} ergs cm^{-2} s^{-1} Å^{-1} (Mégessier 1995). Many alternate and subtly different definitions are possible, but all ultimately relate back to Vega and to several careful, independent determinations of the absolute spectrophotometry of Vega made in the 1970s. These determinations of the fundamental Vega flux are compared and reviewed by Hayes (1985).

Simple, relatively unambiguous definitions of the flux corresponding to observed magnitudes in various photometric bands have a number of advantages. First is the ability to relate the flux in one photometric system to that in another without recourse to a host of empirical photometric transformations. Second, use of a single photometric scale allows easy computation of the corresponding absolute fluxes in different bands. These fluxes in turn possess a known relation to independent photometric or spectrophotometric fluxes at other wavelengths. For example, optical fluxes of a source can be directly compared with its flux at wavelengths from the EUV to the near-IR or beyond. Third, in cases for which reliable stellar model atmospheres exist, as they do for DA (pure-hydrogen) white dwarfs, it is possible to compute synthetic magnitudes and colors at an accuracy supported by the models, which we demonstrate can approach 1% in most instances.

DA white dwarfs have a number of properties that make them excellent candidates for use as flux standards (Holberg 1982; Holberg et al. 1991). First, it is possible, over wide ranges of temperature and gravity, to calculate model atmospheres that have repeatedly been shown to accurately represent both the continuum flux distributions and the detailed line profiles of these stars. A primary reason for this is that these stars (at least for those with $T_{\rm eff}$ in excess of 14,000 K) have fully radiative, pure-hydrogen

[1] Lunar and Planetary Laboratory, University of Arizona, Sonett Spaces Sciences Building, 1541 East University Boulevard, Tucson, AZ 85721-0063; holberg@argus.lpl.arizona.edu.

[2] Département de Physique, Université de Montréal, C.P. 6128, Succursale Centre-Ville, Montréal, QC H3C 3J7, Canada; bergeron@astro.umontreal.ca.

photospheres whose opacity sources can be calculated to high precision. Thus, the model atmospheres of these stars can be completely specified by only an effective temperature ($T_{\rm eff}$) and a surface gravity ($\log g$), together with an appropriate monochromatic flux normalization. Moreover, these two photospheric parameters can be determined to considerable precision by a detailed spectroscopic analysis of the Balmer line profiles in a process that is effectively independent of any relative or absolute photometry. (See Liebert et al. [2005] for an excellent discussion of the current state of the analysis of Balmer lines in DA white dwarfs.)

In addition to their intrinsic properties, DA white dwarfs possess a number of other attributes that also make them ideal calibration standards. These include photometric stability, generally low levels of interstellar reddening, and (for the hotter DA stars) energy distributions that can usefully be used from the EUV to the near-IR bands. One further property, which we make extensive use of, is that these stars cover a wide range of $T_{\rm eff}$ and $\log g$. As a result, their energy distributions exhibit strong wavelength dependencies, particularly at wavelengths shortward of their peak flux peaks. This permits a test of synthetic photometry for stars having markedly different energy distributions and wide ranges of color.

Not all DA white dwarfs meet these criteria or are ideally suited to be standard stars. Some important caveats include the possibility of unresolved low-mass companions, relatively high levels of heavy-element abundance in some of the hotter DA stars, low levels of photometric variability at $T_{\rm eff}$ between 11,000 and 12,500 K (the ZZ Ceti stars), and, in rare cases, possible circumstellar material. In addition, there is also the possibility of photospheric He enrichment in cool DA stars below 10,000 K, where He would not be directly evident in spectra. In most instances, however, these situations are easily recognized, and such stars can be either avoided or used with caution.

The basic strategy we follow in this paper is to first use Vega and the four fundamental *HST* white dwarfs (or the subset of these stars for which observed photometry exists) to define a set of self-consistent photometric zero points for the *UBVRI*, Strömgren, Two Micron All Sky Survey (2MASS), and Sloan Digital Sky Survey (SDSS) photometric systems. These procedures, which rely directly on the absolutely calibrated stellar fluxes of the *HST* calibration standard stars, are described in § 2. In § 3 we make use of an extensive grid of synthetic photometry, derived from stellar model atmospheres and calibrated with respect to the *HST* photometric scale. This synthetic grid is systematically applied to larger sets of DA white dwarfs that have a wide range of well-defined spectroscopic $T_{\rm eff}$ and $\log g$ values and that have been photometrically observed in each of the above systems. Observed − computed ($O - C$) magnitude differences in each band are calculated, and mean offsets between synthetic and real photometry are determined. In § 4 we compare our results with those obtained by previous investigators and demonstrate applications of synthetic photometry.

2. THE *HST* FLUX SCALE

The widely used absolute photometric calibration of the instruments onboard *HST* (Bohlin 2000; Bohlin et al. 1995) is based primarily on the model atmosphere fluxes from four hot DA (pure-hydrogen) white dwarfs: G191-B2B (WD 0501+527), GD 153 (WD 1254+223), GD 71 (WD 0549+158), and to a limited extent HZ 43 (WD 1314+293). The spectral fluxes of these stars are in turn linked to the absolute flux of Vega through normalization to Landolt's carefully measured V magnitudes (see Bohlin 2000; Bohlin & Gilliland 2004, hereafter BG04) and constitute a self-consistent, absolutely calibrated scale encompassing wavelengths from the optical to the UV near Lyman α. Solar analog stars extend this calibration into the IR (Bohlin et al. 2001). Recently, Bohlin & Gilliland (2004) have obtained spectrophotometry of Vega from 1700 Å to 1.01 μm with the Space Telescope Imaging Spectrograph (STIS), thus directly establishing a single-instrument observational link between Vega, the primary astronomical flux standard, and the *HST* white dwarf standards, which are some 13 mag fainter. Using the Landolt V magnitudes for the *HST* standard white dwarfs and the V-band filter of Cohen et al. (2003a), BG04 have also established a new V magnitude for Vega of $V = +0.026 \pm 0.008$. The absolute flux normalization for Vega on this scale is a monochromatic flux of 3.46×10^{-9} ergs cm^{-2} s^{-1} Å^{-1} $\pm$ 0.7% at 5556 Å from Mégessier (1995). BG04 further establish that Vega and the *HST* white dwarf standards are on the same relative photometric scale, such that the mutual flux distributions and observed magnitudes of Vega and the white dwarfs now agree with one another to within 1% between 5000 and 8000 Å. Furthermore, the absolute photometric calibration of this scale is believed to be accurate to 1% after taking into account the uncertainty in the V magnitude of Vega and the uncertainty of the absolute monochromatic flux of Vega. In this section we verify this aspect of BG04 in the V band and demonstrate that it extends to the other Johnson-Kron-Cousins *UBVRI* filters.

Following BG04, we use the Landolt (1992a, 1992b) Johnson-Kron-Cousins Cerro Tololo Inter-American Observatory filter response functions, as modified for atmospheric transmission by Cohen et al. (2003a), and directly compute the synthetic *UBVRI* magnitudes for both Vega and the four primary *HST* flux standards. For these stars we compute the filter-weighted integrated fluxes,

$$F_S = \frac{\int S(\lambda) f(\lambda) \lambda \, d\lambda}{\int S(\lambda) \lambda \, d\lambda}, \tag{1}$$

where $f(\lambda)$ is the tabulated absolute flux of Vega in ergs cm^{-2} s^{-1} Å^{-1} defined by BG04 and $S(\lambda)$ is the relative response of each filter as given by Cohen et al. (2003a). The integration is over the filter bandpass in wavelength (in angstroms) and the integrated fluxes F_s (in ergs cm^{-2} s^{-1}) are then used to compute synthetic magnitudes in each band as follows:

$$M_S = 2.5 \log (F_S) + C_S, \tag{2}$$

where M_S and C_S are the synthetic magnitudes and numerical flux constants for each band S, respectively. The numerical flux constants are defined such that the synthetic magnitudes match the observed Vega magnitudes in each band. Equation (1) uses a photon flux scale to define integrated fluxes, magnitudes, and filter constants. As pointed out by Bessel et al. (1998, hereafter BCP98) and Maíz Apellániz (2005, hereafter MA05), this definition is most appropriate to photon-counting devices such as photomultiplier tubes and CCD detectors. Alternately, it is possible to use an energy scale by replacing the $\lambda \, d\lambda$ with $d\lambda$ in the numerator and denominator of equation (1). In order to maintain continuity with the prior white dwarf synthetic photometry of Bergeron et al. (1995, hereafter BWB95), we also compute the corresponding energy scale constants. In Table 1 we list, for each band, the adopted observed Vega magnitudes and respective references and the resulting integrated fluxes and flux constants for both the photon (cols. [3] and [4]) and energy (cols. [5] and [6]) fluxes of Vega. The observed *UBVRIJHK*$_s$ magnitudes are taken from the colors of Vega given in BCP98 and the new BG04 V magnitude of Vega. Similarly, the observed Strömgren

TABLE 1
Vega Magnitudes and Filters

		Photon Flux		Energy Flux			
Filters (1)	Obs. Mag. (2)	F_S (ergs cm^{-2} s^{-1}) (3)	Filter Const. (4)	F_S (ergs cm^{-2} s^{-1}) (5)	Filter Const. (6)	Mag. Ref. (7)	Filter Ref. (8)
U	+0.020	3.947×10^{-9}	−20.9892	3.886×10^{-9}	−21.0063	1	2
B	+0.024	6.424×10^{-9}	−20.4565	6.452×10^{-9}	−20.4518	1	2
V	+0.026	3.676×10^{-9}	−21.0607	3.711×10^{-9}	−21.0503	3	2
R	+0.033	2.134×10^{-9}	−21.6439	2.202×10^{-9}	−21.6102	1	2
I	+0.029	1.083×10^{-9}	−22.3848	1.093×10^{-9}	−22.3744	1	2
J	+0.023	3.046×10^{-9}	−23.7677	3.077×10^{-9}	−23.7568	1	4
H	+0.025	1.108×10^{-10}	−24.8641	1.116×10^{-10}	−24.8556	1	4
K_s	+0.026	4.167×10^{-11}	−25.9246	4.193×10^{-11}	−25.9178	1	4
u	+1.357	3.176×10^{-9}	−19.8882	3.179×10^{-9}	−19.8874	5	6
v	+0.189	7.322×10^{-9}	−20.1494	7.323×10^{-9}	−20.1493	5	7
b	+0.029	5.761×10^{-9}	−20.5698	5.768×10^{-9}	−20.5685	5	6
y	+0.026	3.648×10^{-9}	−21.0689	3.651×10^{-9}	−21.0678	5	6

References.—(1) BCP98; (2) Cohen et al. 2003a; (3) BG04; (4) Cohen et al. 2003b; (5) Hauck & Mermilliod 1998; (6) Olsen 1974; (7) Kodaira 1975.

magnitudes of Vega are taken from Hauck & Mermilliod (1998). The *HST* calibration file used is *alpha_lyr_stis_002.fits* (file date 2004 June 15). Also included in Table 1 are corresponding calculations for the Strömgren and 2MASS filters, which are described in more detail in §§ 2.1 and 2.2.

In general, throughout this paper we work directly with magnitudes and avoid the explicit use of colors. The primary reason for this is that it simplifies the comparison of the synthetic photometry with observations and the determination of the various photometric zero points. Another compelling reason is that two very large and deep photometric surveys, 2MASS and the SDSS, now follow the practice of directly reporting observed magnitudes and uncertainties. While in principle it is a simple matter to convert magnitudes and zero points to colors and to mathematically propagate the uncertainties, the reverse, however, is not always possible; i.e., recovering magnitude uncertainties from color uncertainties is often ambiguous.

A convenient way to confirm the consistency of the *HST* flux scale is to directly compare the synthetic and observed magnitudes for the four previously mentioned *HST* reference white dwarfs using the computations described in equations (1) and (2) together with the Vega flux constants. In Table 2 we list our adopted *UBVRI* magnitudes and reference spectra. The observed magnitudes are primarily from published and unpublished Landolt observations. In the cases of HZ 43 and G191-B2B, we have used the revised V magnitudes given in Bohlin (2000). In addition, for HZ 43, which has a nearby dM3.5e companion, observed R and I magnitudes are not available.

In Table 3 we give the $O - C$ magnitude differences for each filter and each white dwarf. The computed magnitudes are based on the STScI CALSPEC reference spectra of each star listed in Table 2 and the Vega filter constants from Table 1. As is evident, there is excellent general agreement between the *BVRI* magnitudes for each star. The mean residuals of these filters are within the photometric uncertainties and are not statistically significant. In particular, the small mean difference between the observed and computed V-band magnitudes (−0.0055) is of the same order as the 1 σ magnitude uncertainties of the four DA white dwarfs given in Bohlin (2000) and is smaller than the +0.008 V-band magnitude uncertainty for Vega quoted in BG04. For consistency with the results of BG04, we therefore adopt $\Delta V = 0.0$. In the case of the U band, the clear (∼8%) discrepancy between observed and calculated is due to the fact that the defined flux and the filter response do not accurately represent the atmospheric cutoff, which effectively describes a real star observed at a real telescope. Table 3 indicates that the consistent agreement demonstrated for V magnitudes by BG04 persists at a similar level between the observed magnitudes of Vega and the four DA white dwarfs for all bands from the B band at 4300 Å to the R band at 8000 Å.

2.1. *Strömgren Photometry*

A considerable amount of narrowband Strömgren *uvby* photometry of white dwarfs was obtained in the 1970s and 1980s. However, only two of the primary *HST* calibration standards, GD 71 and GD 153, have published Strömgren photometry. Of these stars, only GD 153 has multiple independent observations and the full complement of *uvby* observations (see Table 4). We directly compare the Strömgren magnitudes of these two stars and determine the corresponding photometric differences in Table 5. In computing our synthetic Strömgren photometry we follow BWB95 and use the *uby* filters given by Olsen (1974) and the v filter given by Kodaira (1975). Unlike the *UVBRI* photometry, considerable differences are apparent between the results for GD 71 and GD 153, as shown in Table 5. However, it should be

TABLE 2
Observed *UBVRI* Magnitudes of *HST* White Dwarf Standards

Star	U	B	V	R	I	Files
GD 71	11.676	12.783	13.032	13.169	13.334	gd71_mod_005.fits
GD 153	11.860	13.060	13.346	13.484	13.665	gd153_mod_004.fits
G191-B2B	10.240	11.447	11.773	11.927	12.105	G191B2B_mod_004.fits
HZ 43	11.369	12.599	12.909	...	...	hz43_mod_004.fits

TABLE 3
O − C UBVRI Magnitude Differences

Star	ΔU	ΔB	ΔV	ΔR	ΔI
GD 71	+0.098	−0.007	−0.006	−0.009	−0.016
GD 153	+0.045	−0.012	−0.006	−0.011	−0.011
G191-B2B.....	+0.129	+0.000	−0.005	−0.001	−0.013
HZ 43.....	+0.091	−0.010	−0.005	...	...
Mean	+0.075	−0.007	−0.0055	−0.007	−0.013

noted that only a single observation of GD 71 exists, in comparison to the four relatively consistent observations of GD 153 for our Strömgren comparison with Vega. Moreover, a considerable difference exists between the V_{obs} and y_{obs} for GD 71 ($V_{obs} - y_{obs} = -0.099$). Based on these considerations, we rely solely on the GD 153 results and set aside those of GD 71.

2.2. *2MASS Photometry*

The 2MASS Point Source Catalog (PSC) contains JHK_s photometry of over 500 million sources and includes all of the four *HST* primary standard white dwarfs. In the case of HZ 43, however, the results are totally contaminated by the presence of the dM3.5e companion and are not used. The 2MASS magnitudes and uncertainties are shown in Table 6.

As with our *UBVRI* results**,** we compute the JHK_s magnitudes for the three fundamental white dwarfs that have useful fluxes. In doing this we use the 2MASS filters, including atmospheric transmission, defined by Cohen et al. (2003b) and adopt the JHK_s Vega magnitudes (see BCP98) and the Vega flux constants from Table 1. The results of these calculations are summarized in Table 7 as $O - C$ magnitude differences for each star, along with the weighted means for each filter. Again, the agreement is reasonably good, to within a few percent. However, the result for the K_s band is dominated by the relatively large residual for GD 71. It is important to note that our use of Vega as a fundamental JHK_s standard relies on the BG04 extrapolation of the observed Vega flux beyond 8500 Å, which is based on the use of a specific Kurucz model atmosphere at these longer wavelengths. Any changes to this model atmosphere will therefore be directly reflected in our synthetic photometry in these bands.

2.3. *Sloan Digital Sky Survey Photometry*

The SDSS is an ongoing photometric and spectroscopic survey of some 9000 deg^2, primarily in the northern hemisphere (York et al. 2000). The photometric observations with the 2.4 m survey telescope, located at the Apache Point Observatory, are conducted in the *ugriz* filter system (Fukugita et al. 1996). Although Vega and the four fundamental *HST* standards are too bright to be observed in the primary SDSS survey, three of the white dwarfs, GD 71, GD 153, and G191-B2B, have been observed with the 0.5 m Apache Point photometric telescope (PT), which is used to photometrically calibrate the secondary patches of the SDSS survey. The PT magnitudes of these three stars, kindly supplied by S. Kent & D. Tucker (2005, private communication), are used to establish the photometric zero points of the five SDSS bands. In doing this we have used the 2.4 m survey filter-response functions from the SDSS Web site,[3] which are believed to closely approximate those of the main 2.4 m survey telescope.

TABLE 4
Observed Strömgren Magnitudes of *HST* White Dwarf Standards

Star	u	v	b	y	Refs.
GD 71	12.686	...	12.897	13.120	1
GD 153	12.898	13.293	13.226	13.370	1, 2, 3, 4

References.—(1) Wegner 1983; (2) Lacombe & Fontaine 1981; (3) Green et al. 1986; (4) Graham 1972.

TABLE 5
Strömgren *O − C* Magnitudes

Star	Δu	Δv	Δb	Δy
GD 71	+0.085	...	−0.022	+0.074
GD 153	+0.063	+0.085	+0.000	+0.009
Adopted.....	+0.063	+0.085	+0.000	+0.009

The SDSS magnitude system (Fukugita et al. 1996) is defined in terms of AB_ν magnitudes at a frequency ν (in hertz),

$$m_\nu = -2.5 \log\left\{\frac{\int S_\nu f_\nu \, d[\log(\nu)]}{\int S_\nu \, d[\log(\nu)]}\right\} - 48.60, \qquad (3)$$

where f_ν is the flux in ergs cm^{-2} s^{-1} Hz^{-1} and S_ν is the total system response including atmospheric transmission corresponding to an air mass of 1.3 and mirror reflectance, as well as the detector quantum efficiency. We will use this definition of SDSS magnitudes.

AB_ν magnitudes are a defined photometric system that relies only indirectly on Vega, so that $AB = V$, near 5480 Å (Oke & Gunn 1983). In this system there are no explicit filter constants of the type determined in Table 1. Nevertheless, there are photometric zero-point offsets that have to be established with respect to standard stars. Effective Vega AB_ν magnitudes are calculated from the *ugriz* filter functions and the BG04 Vega fluxes. In Table 8 we have computed these AB_ν magnitudes for Vega using equation (3). Similar calculations are possible for GD 71, GD 153, and G191-B2B and provide a direct link to the observed magnitudes and uncertainties for these three stars given in Table 9. The corresponding *ugriz*-band $O - C$ magnitude differences are provided in Table 10, along with the weighted means and the uncertainty of the means for each filter. The observed and calculated magnitudes appear to agree to less than 1% in all filters, with the exception of u. Our $O - C$ difference in u of +0.032 mag corresponds closely with the known zero-point offset of the SDSS u band of +0.04 with respect to the AB flux scale. Moreover, our residuals in the other bands are within the quoted 0.01 mag uncertainty for the observed SDSS bands.[4]

3. EXTERNAL VERIFICATION

In the previous section we considered only the relationship of the four photometric systems to Vega and the four fundamental *HST* white dwarfs, where magnitudes were computed (C) directly from the CALSPEC files at STScI. In this section we shift

[3] See http://www.sdss.org/dr4/instruments/imager/index.html#filters.
[4] See http://www.sdss.org/dr4/algorithms/fluxcal.html#assessment.

TABLE 6
Observed JHK_s Magnitudes of *HST* White Dwarf Standards

Star	J	H	K_s
GD 71	13.728 ± 0.025	13.901 ± 0.035	14.115 ± 0.065
GD 153	14.012 ± 0.025	14.209 ± 0.036	14.308 ± 0.062
G191-B2B.....	12.543 ± 0.021	12.669 ± 0.025	12.764 ± 0.023

TABLE 7
JHK_s $O - C$ Magnitude Differences

Star	ΔJ	ΔH	ΔK_s
GD 71	−0.003	+0.058	+0.17
GD 153	−0.058	+0.023	+0.022
G191-B2B	+0.016	+0.024	+0.021
Mean	−0.0112	+0.0325	+0.0359
Error of mean	0.0135	0.0177	0.0205

TABLE 8
Synthetic SDSS Magnitudes of Vega

Star	u	g	r	i	z
Vega	+0.9284	−0.1025	+0.1460	+0.3656	+0.5335

from the *HST* standards to the use of our grid of synthetic (S) photometry based on DA model atmospheres and examine the photometry of a wider range of DA white dwarfs.

The four *HST* white dwarfs are all relatively hot DA white dwarfs with temperatures between 33,000 and 60,000 K and thus have similar energy distributions. One way to explore the application of the *HST* photometric calibrations to a greater range of temperatures and gravities is to consider larger sets of independent DA white dwarfs. These sets all contain stars for which there are well-established spectroscopic $T_{\rm eff}$ and $\log g$ values, as well as V magnitudes from the literature. In cases for which multiple independent determinations of these parameters exist, we have used weighted means to establish a unique value for each parameter. For example, the star EG 102 (WD 1337+705) has four independent spectroscopic published determinations of its $T_{\rm eff}$ and $\log g$, which we have combined to single values of $T_{\rm eff} = 20{,}464$ K and $\log g = 7.90$, and four magnitude determinations with a mean $V = 12.770$. These parameters are used to interpolate within our synthetic photometric grid to specify the synthetic magnitudes in each band of each white dwarf. The use of these larger sets of DA stars permits a robust external verification of our grid of synthetic DA photometry on stars spanning nearly a decade in effective temperature and gravity. It should be noted that our use of synthetic photometry based on $T_{\rm eff}$ and $\log g$ also effectively removes the need for color terms when comparing results between different photometric systems.

3.1. *Models and Methods*

Our synthetic photometry is an extension of the results of BWB95 and the models used by Liebert et al. (2005). Briefly, this grid is built from our own LTE model atmosphere code (see Bergeron et al. 1992 and references therein)—which includes convective energy transport and hydrogen molecular opacity—up to an effective temperature at which NLTE effects are still negligible and the atmospheres are completely radiative. Above this temperature, we then switch to the TLUSTY and SYNSPEC packages to deal with NLTE effects present at higher temperatures. As discussed in detail by Liebert et al. (2005), we needed to ensure that at the branching point both model atmosphere codes yielded similar atmospheric structures and model spectra. To verify this, I. Hubeny (2001, private communication) kindly calculated for us LTE and NLTE pure-hydrogen models and spectra for $T_{\rm eff} > 20{,}000$ K using TLUSTY and SYNSPEC. After some differences between the LTE TLUSTY code and our own LTE code were understood and resolved, the LTE synthetic spectra obtained from both codes agreed to better than 1% in $T_{\rm eff}$ and 0.02 dex in $\log g$ from $T_{\rm eff} = 20{,}000$ to 90,000 K. Thus, the effective temperature at which the two model grids were matched was set at 20,000 K, where the convective flux is zero and where the LTE approximation holds. The NLTE switch in TLUSTY was then turned on to calculate model spectra above $T_{\rm eff} = 20{,}000$ K, while our own LTE code was used to calculate cooler (convective) models. We thus end up with a homogeneous model grid that consistently includes NLTE effects, as well as convective energy transport and molecular opacity. The full grid contains 342 models, with five levels of gravity from 7.0 to 9.5 in 0.5 dex steps and 57 temperatures ranging from 1500 to 100,000 K, including detailed line profiles for the H I Balmer, Paschen, and Brackett lines. We estimate the model-related uncertainties to be less than 1%.

We use these models to compute a photometric grid[5] following a procedure similar to that described in BWB95. The filters used to define the various photometric bands are identical to those used and described in § 2. In addition to our improved models, we have also modified the relations that define the absolute magnitudes given in BWB95. For example, the absolute magnitudes are no longer tied to the Sun but are calculated directly from the observed white dwarf fluxes predicted at the top of the Earth's atmosphere $f_{\rm obs}(\lambda)$ as follows:

$$f_{\rm obs}(\lambda) = 4\pi\left(\frac{R^2}{D^2}\right)H_\lambda, \tag{4}$$

where H_λ is the white dwarf Eddington flux, R is the radius of the white dwarf defined by the Wood (1995) and Fontaine et al. (2001) mass-radius relations, and D is a stellar distance of 10 pc. The corresponding V magnitude, for example, is then computed from the V-band integrated flux (eq. [2]) and the V-band filter constant from Table 1. In terms of the Eddington flux and the white dwarf radius, the absolute V magnitude M_v becomes

$$M_V = -2.5\log\frac{\int_0^\infty R^2 H_\lambda S_V(\lambda)\,d\lambda}{\int_0^\infty S_V(\lambda)\,d\lambda} + 73.6484. \tag{5}$$

Other quantities contained in the photometric grid include the bolometric luminosity $M_{\rm bol}$, the bolometric correction BC, and the cooling age. The bolometric luminosity and bolometric correction are calculated as follows from the white dwarf luminosity L:

$$L = 4\pi\sigma R^2 T_{\rm eff}^4, \tag{6}$$

where σ is the Stefan-Boltzmann constant,

$$M_{\rm bol} = 2.5\log(L/L_\odot) + M_{V,\odot}, \tag{7}$$

and

$$\mathrm{BC} = M_{\rm bol} - M_V, \tag{8}$$

where $M_{V,\odot} = +4.75$ and $L_\odot = 3.826\times10^{31}$ ergs s^{-1} (Allen 1973). The cooling ages, in years, are calculated using the evolutionary models described above. In Figure 1 we illustrate the differences between the M_v values and those of BWB95 in terms of the M_v versus $V - I$ color-magnitude relations for DA stars.

There are three main differences between our calculations and those of BWB95. First, we make use here of the *HST* spectrum

[5] See http://www.astro.umontreal.ca/~bergeron/CoolingModels.

TABLE 9
OBSERVED SDSS MAGNITUDES OF *HST* WHITE DWARF STANDARDS

Star	u	g	r	i	z
GD 71	12.4382 ± 0.0174	12.7517 ± 0.0111	13.2407 ± 0.0129	13.6115 ± 0.0040	13.9730 ± 0.0186
GD 153	12.6995 ± 0.0405	13.0216 ± 0.0128	13.5729 ± 0.0110	12.9496 ± 0.0096	14.3067 ± 0.0162
G191-B2B	11.0326 ± 0.01672	11.4704 ± 0.00458	12.0069 ± 0.0077	12.3884 ± 0.00458	12.7403 ± 0.0068

for Vega, while BWB95 relied on model fluxes from Castelli & Kurucz (1994) in the optical regions; the largest difference is for the U filter, which is 0.24 mag brighter in our revised calculations. Second, in BWB95 we assumed that each magnitude and color index for Vega were identical to zero, while here we use the measured values given in Table 1; this has a negligible effect in color-color diagrams but does affect the theoretical absolute V magnitude. Third, for the *UBVRI* and JHK_s filters we make use here of the Cohen and 2MASS filter sets, respectively, while in BWB95 we relied on the Johnson-Cousins *UBVRI* transmission functions from Bessell (1990) and those of the Johnson-Glass *JHK* system from Bessell & Brett (1988). In what follows, we distinguish between the computed (C) photometry of individual stars discussed in § 2 and the application of our grid of synthetic (S) photometry. We will use the term $O - S$ to refer to the differences between our observed and synthetic photometry.

3.2. *UBRI Comparison*

We have identified a set of 34 DA white dwarfs that possess a full complement of high-quality *UBVRI* photometry, the bulk of which comes from Landolt (1992a, 1992b) and Bergeron et al. (2001). Each of these stars also possesses a well-determined spectroscopic temperature and gravity, and its synthetic V magnitude has been normalized to the *observed mean V magnitude* of each star. The range of effective temperatures extends from 5100 to 61,000 K, and the mean photometric distance for this set of stars is 27 pc. The observed *UBRI* magnitudes have not been corrected for the mean offset magnitudes determined in Table 3. In Table 11 we show our adopted $T_{\rm eff}$, log g, and $V_{\rm obs}$ values along with the $O - S$ residuals and photometric references for each star. Also shown are the simple mean and weighted mean residuals for the sample as well as the standard deviation of the sample. As is evident, the weighted mean *UBRI* residuals in each band (except U) are reassuringly small, below 0.01 mag. The standard deviations for each band are also low, 0.02–0.03 mag, about what is expected from the observational uncertainties alone.

It should be pointed out, however, that for cool DA stars ($T_{\rm eff} < 10{,}000$ K) spectroscopic gravities have an inherent uncertainty due to the possible presence of photospheric helium, which possesses no spectroscopic signature at these temperatures. This can lead to an overestimation of log g. We have investigated possible photometric biases associated with He in cool DA stars by separately computing $O - S$ means for cool DAs in Tables 11 and 12. With the possible exception of the I-band ($\Delta I_{\rm cool} = +0.0380$) and the u-band Strömgren filter ($\Delta u_{\rm cool} = +0.0193$), we find no significant differences between cool and hot DA stars.

TABLE 10
SDSS $O - C$ MAGNITUDES

Star	Δu	Δg	Δr	Δi	Δz
GD 71	+0.0156	−0.0087	−0.0196	−0.0164	−0.0060
GD 153	+0.0413	−0.0437	−0.0033	−0.0022	+0.0002
G191-B2B	+0.0452	+0.0038	+0.0008	−0.0050	−0.0123
Simple mean	+0.0338	−0.0163	−0.0075	−0.0080	−0.0060
Weighted mean	+0.0317	−0.0023	−0.0044	−0.0108	−0.0098
Error of mean	0.0116	0.0040	0.0057	0.0029	0.0059

As noted in § 3.1, our synthetic photometry grid differs in a number of respects from the results of BWB95. In Figure 2 we illustrate the nature of these differences with respect to the $U - B$ versus $B - V$ color-color diagram. In Figure 2 the dark curve represents the prior colors for log $g = 8.0$ from BWB95. It should be noted that the U band in this plot is calculated from the modified U-band filter of MA05 (see discussion in § 4.1) and not the Cohen U-band filter.

3.3. *Strömgren Comparison*

We compare the observed Strömgren *uvby* magnitudes for a set of 37 DA stars that cover a broad range of effective temperatures, from 7000 to 55,000 K at a mean photometric distance of 37 pc. Strömgren photometry is generally reported as y, $b - y$,

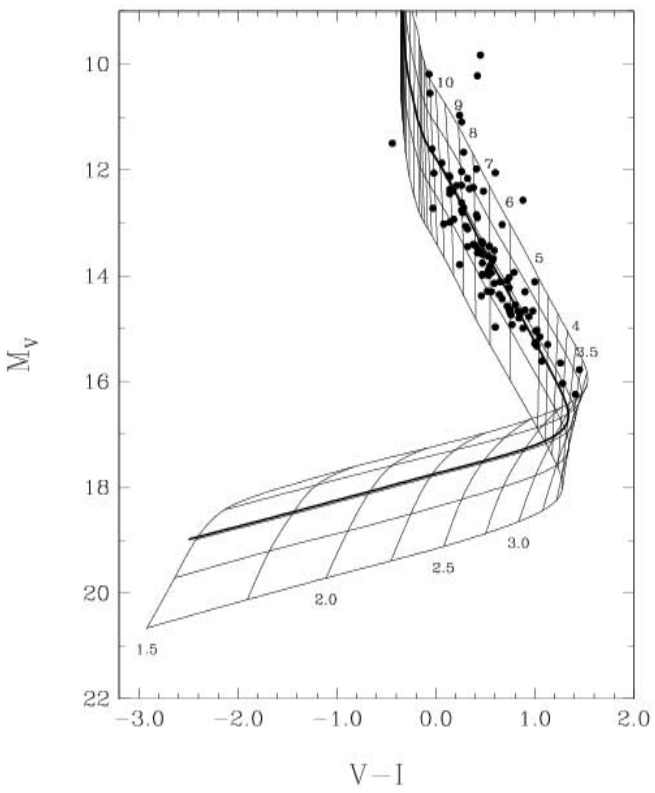

FIG. 1.—M_v vs. $V - I$ color-magnitude diagram for DA stars. For comparison with the results of BWB95, the dark curve illustrates the trace for log $g = 8.0$ DA stars from the BWB95 grid. The labeled vertical trending curves are lines of constant $T_{\rm eff}$ (in units of 1000 K), and the near orthogonal curves are lines of constant gravity, which ascend log $g = 9.0$, 8.5, 8.0, 7.5, and 7.0. The data points are those stars with trigonometric parallaxes from Bergeron et al. (2001).

TABLE 11
$O - S$ Magnitudes of *UBVRI* Comparison White Dwarfs

Star	V_{obs}	T_{eff}	log g	ΔU	ΔB	ΔR	ΔI	Ref.
WD 0208+396	14.514	7320	8.02	0.1221	−0.0104	−0.0239	0.0157	1
WD 0227+050	12.799	19073	7.777	0.0951	0.0096	0.0021	0.0008	2
WD 0310−688	11.366	16181	8.062	0.0986	0.0084	0.0007	−0.0009	3
WD 0346−011	14.063	43102	9.092	0.1046	0.0005	−0.0040	−0.0042	2
WD 0413−077	9.527	16402	7.852	0.1392	0.0298	−0.0045	−0.0565	4
WD 0501+527	11.727	58100	7.45	0.0958	−0.0048	0.0045	−0.0061	5
WD 0549+158	13.032	33753	7.664	0.1157	0.0042	−0.0042	−0.0118	2
WD 0839−327	11.846	9393	7.955	0.0923	0.0134	−0.0025	0.0063	3
WD 0930+294	15.95	8330	8.38	0.0737	−0.0032	0.0388	0.0612	1
WD 1105−048	13.059	15576	7.805	0.0689	0.0102	0.0032	0.0056	2
WD 1121+216	14.237	7470	8.20	0.0743	−0.0236	−0.0087	−0.0097	1
WD 1134+300	12.493	21268	8.546	0.0556	−0.0181	−0.0034	−0.0037	5
WD 1236−495	13.782	11730	8.81	0.0833	0.0015	−0.0127	−0.0138	3
WD 1254+223	13.346	39621	7.83	0.0900	−0.0055	−0.0065	−0.0055	5
WD 1257+278	15.41	8734	8.329	0.1181	0.0196	−0.0161	0.0199	1
WD 1337+705	12.77	20464	7.90	0.0650	−0.0054	−0.0006	−0.0108	5
WD 1455+298	15.60	7382	7.962	0.0392	−0.0285	0.0051	0.0593	1
WD 1609+135	15.098	9323	8.646	0.0959	0.0115	0.0144	0.0095	1
WD 1615−154	13.422	29833	8.083	0.0540	0.0070	−0.0030	−0.0119	2
WD 1620−391	11.008	24406	8.099	0.0819	0.0118	0.0025	0.0039	3
WD 1625+093	16.136	6870	8.44	0.0774	−0.0153	0.0080	0.0522	1
WD 1633+433	14.83	6669	8.177	0.1155	0.0080	0.0277	0.0543	1
WD 1637+335	14.658	10147	8.169	0.0749	0.0043	−0.0167	−0.0170	1
WD 1655+215	14.102	9313	8.203	0.1069	0.0193	0.0266	0.0447	1
WD 1824+040	13.889	14795	7.68	0.1508	0.0517	−0.0366	−0.0688	2
WD 1855+338	14.635	11950	8.35	0.1130	0.0036	−0.0263	0.0107	1
WD 2007−303	12.206	15152	8.35	0.0818	−0.0155	0.0663	0.0719	3
WD 2105−820	13.596	10200	8.23	0.1128	0.0380	0.0136	0.0019	1
WD 2149+021	12.739	17653	7.994	0.0726	0.0121	0.0018	0.0015	2
WD 2240−017	16.205	9150	8.10	0.0921	0.0255	0.0120	0.0187	6
WD 2246+223	14.358	10648	8.804	0.0723	0.0013	0.0188	−0.0018	1
WD 2248+293	15.528	5520	7.49	0.1829	0.0057	0.0381	0.0954	1
WD 2309+105	13.094	54410	7.90	0.1120	−0.0070	−0.0016	−0.0143	2
WD 2326+049	13.03	11817	8.146	0.0262	−0.0164	−0.0209	−0.0343	7
Weighted mean				0.0915	0.0069	0.0018	−0.0014	
Unc. of mean				0.0008	0.0005	0.0004	0.0009	
Simple mean				0.0928	0.0042	0.0027	0.0077	
Std. dev.				0.0310	0.0170	0.0203	0.0343	

References.—(1) Bergeron et al. 2001; (2) Landolt 1992a; (3) Landolt 1992b; (4) Oswalt et al. 1996; (5) A. U. Landolt 1991, private communication; (6) Bergeron et al. 1997; (7) Bessell 1990.

and $u - b$ colors and sometimes $m_1 = (v - b) - (b - y)$. Consequently, the v band, which straddles the Hγ line, is not always available for all stars. In most instances we have, for the sake of reliability, selected stars that have two or more independent (and consistent) observations made by different observers and averaged the observed colors before determining the magnitudes. GD 71 (WD 0549+158), one of two *HST* standards, is the only exception, since it possesses just a single published result (Wegner 1983). We have also not used the $u - b$ colors of Green et al. (1986), since these show strong differences with other observers.

In Table 12 we show our adopted T_{eff}, log g, and y_{obs} values along with the $O - S$ residuals for each star and each band and the references for the Strömgren photometry. Also shown are the simple means and the standard deviations of the sample. As is evident, the mean the *uvb* residuals in each band are modest, approximately −0.01. The standard deviations are somewhat larger than for the *UBVRI* photometry. This reflects the more heterogeneous nature and lower accuracy of the Strömgren photometry.

It is generally assumed that $y_{obs} = V_{obs}$. Indeed, V_{obs} and not y_{obs} is often what is reported in conjunction with Strömgren colors. However, this is not the case for white dwarfs, where y_{obs} is given. We have normalized our synthetic magnitudes to y_{obs}, so any offset in y_{obs} will be reflected in the residuals of the other bands. The $O - C$ value for y in Table 5 was found to be +0.009, a result that is not statistically significant given the uncertainty in y_{obs} for a single star (GD 153). The equivalence between V_{obs} and y_{obs} can be investigated further, since we possess V_{obs} and y_{obs} for 18 DA stars in common between Tables 11 and 12. The mean difference ($V_{obs} - y_{obs}$) for these 18 stars is +0.0124 ± 0.007. If we adopt this as the zero-point offset for y_{obs}, the mean values of Δu, Δv, and Δb become −0.0019, −0.0013, and −0.0014, respectively. We therefore adopt the relation between V_{obs} and y_{obs} as being $V_{obs} = y_{obs} + 0.0124$.

3.4. *2MASS Comparison*

We have recovered the observed 2MASS magnitudes and associated uncertainties for a set of 175 DA stars from the 2MASS PSC. Efforts were made to exclude stars for which unresolved low-luminosity companions had been previously noted, as well as those with known magnetic fields, since our model grid does not incorporate magnetic fields. We also required good determinations of the V magnitude of each star. This sample included

TABLE 12
$O - S$ Magnitudes of Strömgren Comparison White Dwarfs

Star	y_{obs}	T_{eff}	log g	Δu	Δv	Δb	Refs.
WD 0227+050	12.8	19073	7.777	0.0017	0.0003	−0.0058	1, 2, 3, 4
WD 0310−688	11.35	16181	8.062	0.0218	−0.0828	−0.0208	4, 5
WD 0413−077	9.53	16402	7.752	−0.0456	−0.0213	−0.0126	1, 3, 4
WD 0549+158	13.12	33753	7.664	−0.0605	...	−0.0992	1
WD 0839−327	11.86	9393	7.955	0.0340	0.0006	0.0051	5, 6
WD 1031−114	13.00	25312	7.815	0.0228	−0.0028	−0.0033	3, 4, 6
WD 1042−690	12.80	21380	7.864	0.0428	−0.0132	0.0085	4, 5, 7
WD 1105−048	13.06	15576	7.805	−0.0189	−0.0265	−0.0169	1, 3, 6
WD 1236−495	13.76	11730	8.81	0.0647	−0.0066	−0.0158	4, 5
WD 1244+149	15.91	10684	8.06	−0.0420	−0.0433	−0.0278	2, 3
WD 1254+223	13.37	39621	7.83	−0.0231	0.0756	−0.0137	1, 2, 3, 8
WD 1317+453	14.06	13335	7.383	−0.0817	...	−0.0297	1, 3, 8
WD 1323−514	14.40	18713	7.87	−0.0753	−0.0567	−0.038	4, 5
WD 1327−083	12.33	13762	7.876	−0.1226	−0.0731	−0.0466	1, 3, 4, 8
WD 1337+705	12.80	20464	7.9	−0.0309	−0.0347	−0.0341	3, 8
WD 1407−475	14.33	22286	7.812	0.0649	0.0591	0.0109	4, 5
WD 1415+132	15.37	34179	7.38	0.0330	0.0035	−0.0119	3, 8
WD 1509+322	14.08	14460	7.991	−0.0887	−0.0259	−0.0204	1, 9
WD 1539−035	15.23	10080	8.30	0.0619	−0.0261	...	3, 8
WD 1559+369	14.35	11160	8.042	0.0336	0.0012	−0.0136	1, 8, 10
WD 1606+422	13.87	11320	7.12	−0.2058	−0.0078	−0.0174	1, 8
WD 1609+135	15.10	9323	8.646	0.0633	−0.0505	0.0227	1, 2
WD 1615−154	13.47	29833	8.083	−0.0424	−0.0429	−0.0258	2, 4, 8
WD 1620−391	10.99	24406	8.099	0.0149	−0.0391	−0.0112	4, 5
WD 1633+433	14.84	6669	8.177	0.0243	0.0313	0.0037	1, 2
WD 1655+215	14.12	9313	8.203	0.0270	−0.0219	−0.0226	3, 8
WD 1716+020	14.35	13470	8.11	0.0516	−0.0274	0.0024	4, 8
WD 1840+042	14.82	9090	8.19	−0.0079	...	0.0065	1, 8
WD 1911+135	14.05	13769	7.831	−0.0300	0.0223	−0.0273	1, 8
WD 1953−011	13.69	7932	8.412	0.0186	−0.0118	−0.0069	1, 4, 8
WD 2032+248	11.53	19933	7.836	−0.0997	−0.0512	−0.0226	1, 2, 8
WD 2105−820	13.60	10200	8.23	0.0800	−0.0227	0.0007	4, 5
WD 2149+021	12.80	17653	7.994	−0.1602	−0.0879	−0.0361	1, 2
WD 2226+061	14.71	15282	7.62	−0.0940	...	0.0099	1, 9
WD 2309+105	13.08	54410	7.90	−0.0393	...	−0.0511	1, 5, 9
WD 2326+049	13.03	11817	8.146	0.0038	...	−0.0155	1, 10
WD 2341+322	12.97	12574	7.93	0.0745	0.1871	0.0669	2, 3, 8
Mean				−0.0143	−0.0107	−0.0138	
Standard Dev.				0.0681	0.0517	0.0257	

References.—(1) Wegner 1983; (2) Lacombe & Fontaine 1981; (3) Green et al. 1986; (4) Wegner 1979; (5) Bessell & Wickramasinghe 1978; (6) Koester & Weidemann 1982; (7) Kawka et al. 2002; (8) Graham 1972; (9) Green 1977; (10) McCook & Sion (1999).

stars with T_{eff} values of 4200–93,000 K and log g values from 7.0 to 9.1. The mean photometric distance of this set of stars is 60 pc. Synthetic JHK_s magnitudes, normalized to the observed V-band residuals, were then computed for each star and used to determine the corresponding $O - S$ residual magnitudes. An examination of the distribution of $O - S$ magnitudes as a function of stellar effective temperature for each band showed no dependence of the residuals on T_{eff}, which could, for example, arise from model bias. In Figure 3 we plot the distribution of JHK_s residuals. Ideally, this distribution should have a zero mean and a width that reflects the joint uncertainties in the input spectroscopic parameters and the observational uncertainties in the PSC. In order to minimize the effect of unrecognized low-luminosity companions the centroid of the frequency distribution in each band was determined by fitting a Gaussian distribution. The small tail of negative outliers in each band may well represent stars with previously unknown very late M- or L-type companions (see Holberg & Margargal 2005).

Note that the number of stars is not the same for each filter. This is due to the fact that we used only stars whose 2MASS flux uncertainties met the greater than 10 σ uncertainty threshold of the 2MASS PSC. This criterion effectively limited the number of H and K_s determinations. In Table 13 we give the number of stars in each filter, the sample means, along with the uncertainties of the mean, the Gaussian centroids, and the full width at half-maximum (FWHM). A complete listing of the 2MASS photometry and the adopted T_{eff} and log g values are given in the online version of the table.

3.5. *SDSS Comparison*

In order to facilitate a comparison of SDSS magnitudes with the *HST* photometric scale, we have identified two sets of DA white dwarfs obtained from the DR4 *SkyServer*[6] online database. The primary reason for two comparison sets is that the number of stars with reliable V-band fluxes is limited, and the uncertainties of most V-band magnitudes are several times larger than those of the SDSS photometry. Consequently, we first investigate any

[6] See http://cas.sdss.org/dr4/en/.

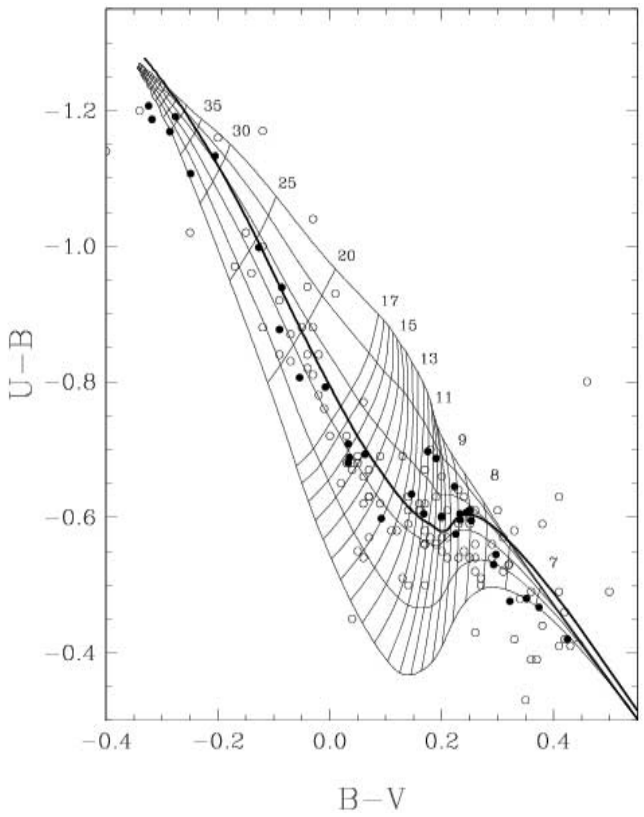

FIG. 2.—Comparison of our new $U-B$ vs. $B-V$ color-color diagram for DA stars (*light curves*) with a corresponding $\log g = 8.0$ (*dark curve*) from the BWB95 grid. The diagonally trending curves are traces of constant gravity ascending from $\log g = 7.0$ to 9.0 in steps of 0.5 dex, while the labeled near orthogonal curves are traces of constant $T_{\rm eff}$ (in units of 1000 K). The filled circles are taken from the data in Table 11, while the open circles are from the Yale parallaxes of van Altena et al. (1994; see BWB95).

TABLE 13

OBSERVED 2MASS MAGNITUDES AND MODEL INPUT PARAMETERS

WD	$T_{\rm eff}$	$\log g$	V	J	H	K
WD 0004+330	49639	7.71	13.847	14.51	14.648	14.728
WD 0009+501	6540	8.23	14.375	13.49	13.249	13.191
WD 0011+000	9610	8.4	15.32	15.148	15.214	15.101
WD 0027−636	62394	7.9	15.314	16.018	16.08	15.808
WD 0033+016	10700	8.66	15.61	15.65	15.522	16.119
WD 0037+312	48856	7.83	14.66	15.359	15.478	15.478
WD 0048+202	20340	7.97	15.36	15.878	15.952	...
WD 0050−332	35326	7.92	13.36	14.004	14.174	14.318
WD 0058−044	16630	8	15.38	15.854	15.845	15.946
WD 0101+048	8080	7.55	14.023	13.504	13.396	13.418
WD 0102+095	24741	7.87	14.46	15.019	15.073	15.004

NOTES.—Table 13 is published in its entirety in the electronic edition of the *Astronomical Journal*. A portion is shown here for guidance regarding its form and content. Statistical summary of $O-S$ results: J band—175 stars, mean of residuals = −0.015, centroid = −0.014, FWHM = 0.059; H band—115 stars, mean of residuals = +0.011, centroid = +0.006, FWHM = 0.059; K_s band—75 stars, mean of residuals = +0.005, centroid = +0.008, FWHM = 0.037.

offsets between V-band and g-band photometry and then separately compare the remaining SDSS bands with respect to the g band.

The first set consists of 107 DA stars that have well-established spectroscopic $T_{\rm eff}$ and $\log g$ estimates, with the added constraint of well-determined V magnitudes. This set is used to make an initial evaluation of the observed and synthetic g-band magnitudes as follows. An apparent synthetic g-band magnitude is estimated for each star from the relation $g = V - (M_v - M_g)$, where M_v and M_g are the synthetic absolute magnitudes interpolated from within our photometric grid and V is the observed V magnitude. This effectively normalizes the g band to the *HST* photometric scale through the observed V magnitudes of each star. In Figure 4 we show the $O-S$ frequency distribution of the g-band residuals and a Gaussian fit to this distribution. As is evident in Figure 4, there is a small but significant offset between the observed and synthetic g-band magnitudes. The zero offset, as determined from the centroid of the Gaussian, is found to be -0.0204 ± 0.0038 mag. This is significantly larger than the weighted mean of the $O-C$ differences for g of -0.0023 ± 0.0040, obtained from the three *HST* standard stars in § 2.3 (Table 10), but is in better agreement with the simple mean of −0.0163. The former value is dominated by the small statistical uncertainty for G191-B2B, while the latter is primarily a result of the large $O-C$ value for GD 153. Our interpretation of the difference between our synthetic $O-S$ offset between V and g is that some of it may well arise from our definition of M_v coupled with the nominal 1% uncertainty in the SDSS g-band zero point. Nevertheless, the $O-C$ values for g could well be biased by the observed g-band fluxes for either GD 153 or G191-B2B or both. We therefore adopt the latter (*HST*) estimate of the g-band offset of −0.0023. The FWHM of the distribution is 0.09 mag, the bulk of which comes from V-band uncertainties, which are estimated at ∼0.03 mag per star. A complete listing of the SDSS photometry and the adopted $T_{\rm eff}$ and $\log g$ values are given in the online version of Table 14.

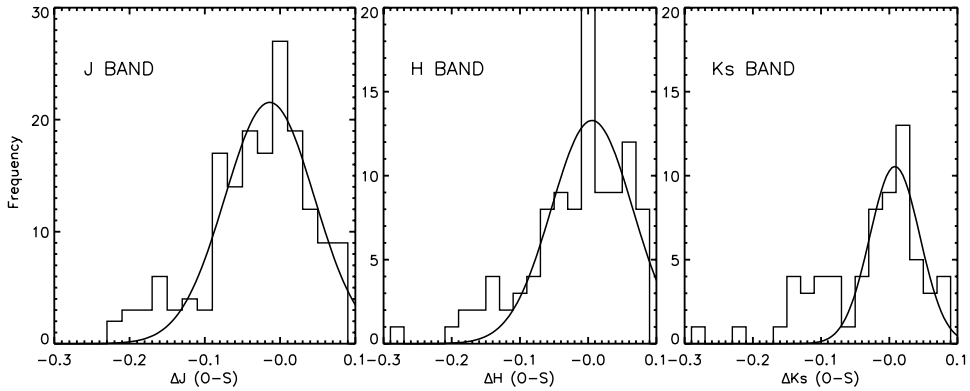

FIG. 3.—Frequency distributions of the JHK_s $O-S$ residuals and corresponding Gaussian fits. The synthetic magnitudes are normalized to the V-band magnitudes.

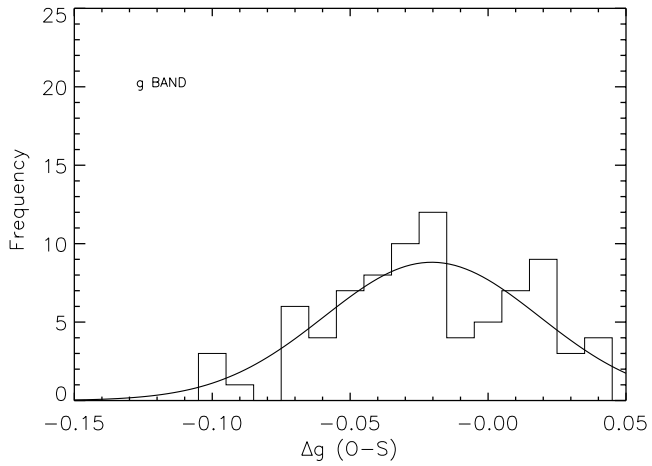

FIG. 4.—Frequency distribution of the $O - S$ g-band residuals for 107 DA white dwarfs and the Gaussian fit. The synthetic g magnitudes are normalized with respect to V-band photometry.

We have identified a second, larger set of 175 previous known DA stars from the SDSS DR4 through the use of precise coordinates from the White Dwarf Database.[7] As before, unresolved binaries and magnetic stars were avoided. The *ugriz* point-spread function magnitudes and associated uncertainties were obtained from *SkyServer*. We included lower magnitude limits, since several of our stars saturate in the g band at around $g \sim 13.55$ ($V \sim 13.7$). For several additional stars there were obvious but unexplained flux deficits that exceeded a magnitude in isolated bands; these stars were also excluded. The synthetic *uriz* magnitudes were self-normalized using the observed g-band flux in the computation of the $O - S$ flux differences computed for the *uriz*-band magnitudes. The frequency distributions of the differential magnitudes in each band are plotted in Figure 5 and summarized in Table 14. As before, we have determined the magnitude offsets in each band from the centroids of the Gaussian fits to the frequency distributions of the residuals.

It should be emphasized here that our sample of SDSS white dwarfs is based primarily on bright white dwarfs that have been the subject of prior spectroscopic study. Consequently, this sample is relatively nearby (the mean distance is 140 pc) and not subject to significant interstellar reddening. A similar calculation of residuals, based on the subsample of the 70 stars closer than 70 pc, showed no significant differences from the results for the entire sample. The bulk of all white dwarfs contained in the SDSS are much fainter and more distant, and the resulting magnitudes and colors will contain significant reddening. Therefore, any use of our synthetic photometry on this fainter sample needs to include appropriate reddening corrections. In Figure 6 we illustrate the $u - g$ versus $g - r$ color-color diagram for the stars in Table 14 with respect to our synthetic grid.

[7] See http://procyon.lpl.arizona.edu.

4. DISCUSSION AND CONCLUSIONS

In Table 15 we present our adopted differential magnitude corrections for each of the photometric bands discussed in this paper. The differential magnitudes for the *UBVRI* and JHK_s bands are based on our adoption of $\Delta V = 0.0$ and the weighted means of Table 11 and the centroids of Table 13, respectively. For the Strömgren bands we have included the $V_{\rm obs} - y_{\rm obs} = +0.0124$ offset of our means (§ 3.3) from Table 12. For the SDSS bands we adopt $\Delta g = -0.0023$ and the centroids from Table 14. The sense of all these differential corrections (ΔM) is

$$M_{\rm obs} = M_{\rm synth} + \Delta M. \quad (9)$$

These differential corrections have been applied to the monochromatic absolute fluxes in Table 15. For the purposes of comparison with previous results, the adapted wavelengths in Table 15 were chosen to correspond to the isophototal wavelengths for the *UBVRI* and JHK_s bands defined in Cohen et al. (2003a, 2003b), respectively. The corresponding Cohen et al. isophototal fluxes (including Cohen's zero-point corrections for the JHK_s bands) are also shown in Table 15. In the case of the Strömgren bands, we have used the wavelength centroids and monochromatic fluxes of Gray (1998).

4.1. *Comparison with Previous Results*

The most relevant independent results that compare with our $UBVRIJHK_s$ bands are from Cohen et al. (2003a, 2003b). With respect to the Cohen absolute fluxes, the largest difference occurs in the U band, where our flux is 7% lower. The *BVR* bands agree very well, to within 0.5%. Our $IJHK_s$ bands, however, are

TABLE 14
OBSERVED SDSS MAGNITUDES AND MODEL INPUT PARAMETERS

WD	$T_{\rm eff}$	log g	u	g	r	i	z
WD 0011+000	9610	8.4	15.754	15.366	15.433	15.501	15.686
WD 0019+150	30800	8.1	16.757	17.062	17.518	17.859	18.196
WD 0108+143	9195	8.54	17.281	16.916	16.985	17.037	17.157
WD 0343−007	65605	7.683	14.205	14.652	15.123	15.495	15.802
WD 0346−011.....	41676	9.134	13.383	13.823	14.282	14.632	14.999
WD 0742+231	60000	7.66	16.539	16.967	17.429	17.818	18.185
WD 0752+365	7700	8.19	16.586	16.16	16.05	16.054	16.17
WD 0802+413	48439	7.457	14.516	14.935	15.432	15.776	16.117
WD 0816+297	16655	7.837	15.813	15.678	15.978	16.229	16.55
WD 0816+387	7570	8.19	17.034	16.611	16.498	16.47	16.538

NOTES.—Table 14 is published in its entirety in the electronic edition of the *Astronomical Journal*. A portion is shown here for guidance regarding its form and content. Statistical summary of $O - S$ results: u band—175 stars, mean of residuals = +0.0499, centroid = +0.0394, FWHM = 0.0380; g band—107 stars, mean of residuals = +0.0023, centroid = −0.0204, FWHM = 0.09; r band—175 stars, mean of residuals = +0.0010, centroid = −0.0056, FWHM = 0.0308; i band—175 stars, mean of residuals = −0.0135, centroid = −0.0190, FWHM = 0.0308; z band–175 stars, mean of residuals = −0.0260, centroid = +0.0300, FWHM = 0.0414.

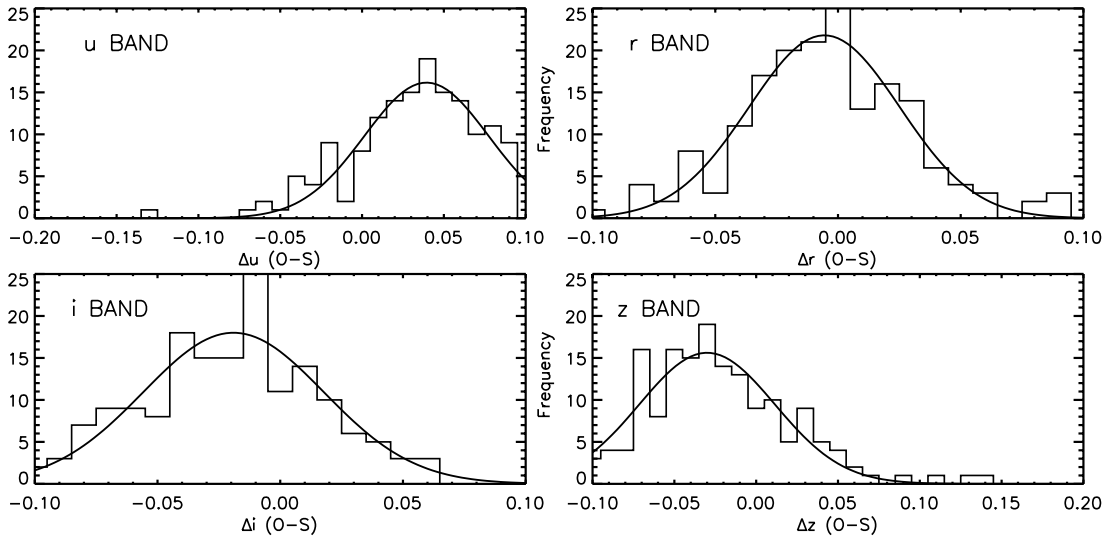

FIG. 5.—Frequency distributions of the *uriz* $O - S$ residuals and corresponding Gaussian fits for 175 DA stars. The synthetic magnitudes are normalized to the *g*-band magnitudes.

systematically lower by slightly less than 1% than those of Cohen. As pointed out by BG04, this latter difference is primarily the result of the different Vega model employed by Cohen and the *HST* Vega fluxes of BG04 used here. The former rely on a Vega model, which is somewhat cooler (9400 K) than the model (9550 K) used by BG04 to extend the *HST* Vega fluxes beyond 8500 Å. If instead we use the cooler Cohen (1993) model, these differences largely disappear. Since we use the Cohen et al. $UBVRIJHK_s$ filters, our agreement with the results of Cohen et al. is to be expected. Cohen et al. have already demonstrated the applicability of their results to main-sequence stars. We basically extend this to DA white dwarfs. The primary systematic difference is our use of the BG04 Vega spectrum and the *HST* photometric scale.

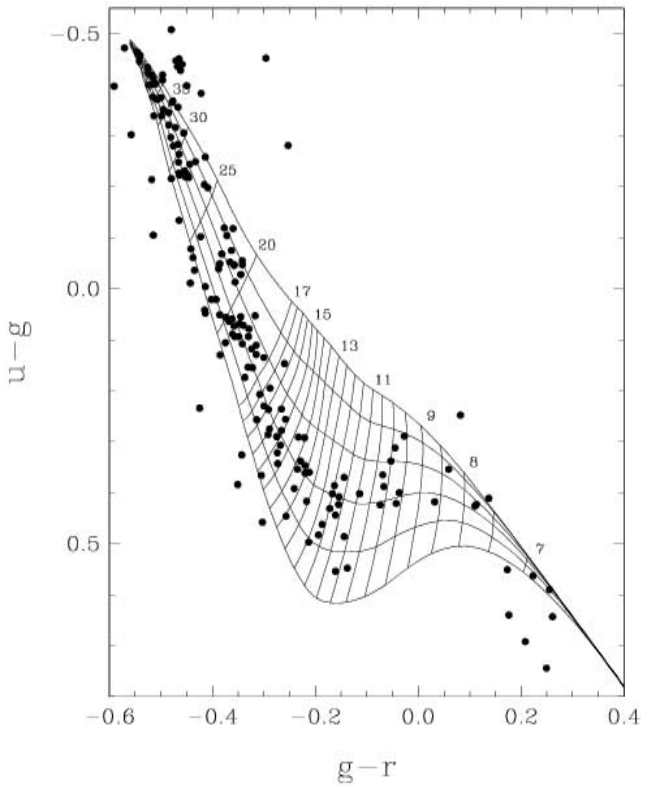

FIG. 6.—Comparison of our theoretical $u - g$ vs. $g - r$ colors with the 175 SDSS DA white dwarfs from Table 14.

In contrast to our agreement with Cohen et al. (2003a, 2003b), we find considerable differences with respect to the recent photometric calibration of the $UBVRIJHK_s$ bands by BCP98. In comparing our results with BCP98, we compute the zero-magnitude fluxes using the same set of effective wavelengths as BCP98. Our *U*-band flux is 28% lower than that of BCP98, while the remaining bands are 3%–9% higher than BCP98.

Our Strömgren-band results are compared with those of Gray (1998). The respective relative differences for *uvby* are −6%, −29%, +2.9%, and −0.8%. The extremely large differences for the *v* band can be attributed to the fact that this filter spans the Hγ line, which in white dwarfs can be quite large. Our *v*-band calibration for Vega and GD 153 are consistent to within 9%, and our external comparison of 35 DA white dwarfs is good to better than 1%, indicating that our synthetic *v*-band photometry is a valid representation of the observed photometry for these stars.

MA05 has conducted an analysis similar in many respects to that presented here, in that synthetic and observed photometry are compared for several different photometric systems. Points in common between our work and that of MA05 include detailed examinations of the Johnson *UBV* and Strömgren systems, together with the BG04 Vega flux distribution, to define the absolute calibration of the various systems. Major points of difference involve our exclusive reliance on DA white dwarfs as opposed to the predominant use of bright luminous stars observed with STIS by MA05. In particular, we use model atmosphere-based spectral energy distributions defined by spectroscopically derived effective temperatures and gravities versus MA05's use of bright luminous stars, albeit on the uniform *HST* flux scale. In addition, we work primarily with magnitudes, while MA05 focus on colors and the determination of color zero points, and we use an energy scale as opposed to the systemic use of the photon scale by MA05. Nevertheless, several important conclusions common to both works are evident. These are that high-quality *HST* spectrophotometry can be used to consistently calibrate various photometric systems and that published photometric response curves adequately represent the results of ground-based photometry, with small zero-point offsets. The Johnson *U* band, however, is

TABLE 15
MAGNITUDE OFFSETS AND ZERO-POINT MONOCHROMATIC FLUXES

Band	Mag. Offset (ΔM)	λ_{ref}[a] (Å)	Zero-Mag. F_λ[a]	Alt. Determinations	Ref.
U	+0.0915	3971	3.684×10^{-9}	3.971×10^{-9}	1
B	+0.0069	4481	6.548×10^{-9}	6.562×10^{-9}	1
V	+0.0000	5423	3.804×10^{-9}	3.789×10^{-9}	1
R	+0.0018	6441	2.274×10^{-9}	2.274×10^{-9}	1
I	−0.0014	8071	1.119×10^{-9}	1.129×10^{-9}	1
J	−0.0140	12350	3.106×10^{-10}	$(3.126 \pm 0.055) \times 10^{-10}$	2
H	+0.0060	16620	1.143×10^{-10}	$(1.153 \pm 0.022) \times 10^{-10}$	2
K_s	+0.0080	21590	4.206×10^{-11}	$(4.216 \pm 0.081) \times 10^{-11}$	2
u (Strom.)	−0.0143	3491	1.024×10^{-8}	$(1.172 \pm 0.012) \times 10^{-8}$	3
v (Strom.)	−0.0107	4111	6.115×10^{-9}	$(8.66 \pm 0.09) \times 10^{-9}$	3
b (Strom.)	−0.0138	4662	6.059×10^{-9}	$(5.89 \pm 0.04) \times 10^{-9}$	3
y (Strom.)	−0.0124	5456	3.699×10^{-9}	$(3.73 \pm 0.01) \times 10^{-9}$	3
u (SDSS)	+0.0424	3146	1.1436×10^{-8}	...	
g (SDSS)	−0.0023	4670	4.9804×10^{-9}	...	
r (SDSS)	−0.0032	6156	2.8638×10^{-9}	...	
i (SDSS)	−0.0160	7471	1.9216×10^{-9}	...	
z (SDSS)	−0.0276	8918	1.3343×10^{-9}	...	

[a] Isowavelength and isoflux (in units of ergs cm $^{-2}$ s^{-1} Å^{-1}; see Cohen et al. [2003a, 2003b]).
REFERENCES.—(1) Cohen et al. 2003a; (2) Cohen et al. 2003b; (3) Gray 1998.

a prominent exception and requires either a large zero-point offset or a redefinition of the blue side of the filter functions that limits the short-wavelength response of these filters. MA05 adopted the latter point of view and defined a *U*-band filter with a modified short-wavelength response. We have used this filter and find that a computation of the mean *U*-band offsets for the four *HST* standard stars yields an offset of 0.0 compared to the +0.106 we obtained with an unmodified Cohen *U*-band filter.

4.2. *Applications*

As an example of the type of calculations possible with synthetic fluxes of the type we have described here, we show in Figure 7 a comparison of the $V - g$ versus $B - V$ relation of Rodgers et al. (2006)[8] between the Johnson and SDSS systems. In Figure 7 the dashed lines show the *empirical linear* relation (and 1 σ uncertainties) derived by Rodgers et al. from observations of main-sequence stars. The solid lines show our synthetic photometry (with the offsets given in Table 15) for DA stars with gravities of $\log g = 7.0$, 7.5, 8.0, 8.5, and 9.0. The general agreement is quite good considering the two different types of stars and data sources involved. The major differences can be attributed to the gravity dependence of the white dwarf colors in the region $B - V < +0.3$. Many similar photometric relations can be easily generated from our grid of synthetic photometry.

4.3. *Conclusions*

Using DA white dwarfs, we have calibrated four major photometric systems with respect to the *HST* absolute flux scale. These systems include the Johnson-Kron-Cousins *UBVRI*, the Strömgren *uvby*, the 2MASS JHK_s, and the SDSS *ugriz* filters. Photometric constants are computed directly from Vega for the $UBVRIJHK_s$ and *uvby* filters (Table 1). These constants are shown to produce good agreement between observed and computed photometry for these bands with respect to the four *HST* fundamental white dwarf standards. This establishes the photometric linearity of this system for bands outside *V*. A grid of synthetic photometry for DA white dwarfs, based on these photometric constants, is presented. This grid is systematically compared to observations for large samples of DA white dwarfs, where spectroscopic $T_{\rm eff}$ and $\log g$ values are known. Good agreement between synthetic and observed magnitudes is demonstrated for all but the shortest wavelength bands, *U*, Strömgren *u*, and SDSS *u*, where atmospheric extinction plays a dominant role. Finally, zero-magnitude offsets and zero-magnitude monochromatic fluxes for each band are determined and compared with prior results (Table 15). Our results are in good agreement with those of Cohen et al. (2003a, 2003b), MA05, and Fitzpatrick & Massa (2005), where similar techniques have been applied to luminous stars.

For the SDSS bands, which have defined magnitudes, we have determined the magnitudes of Vega and three of the four *HST* fundamental white dwarf standards. A grid of synthetic photometry is introduced for the *ugriz* bands and directly compared

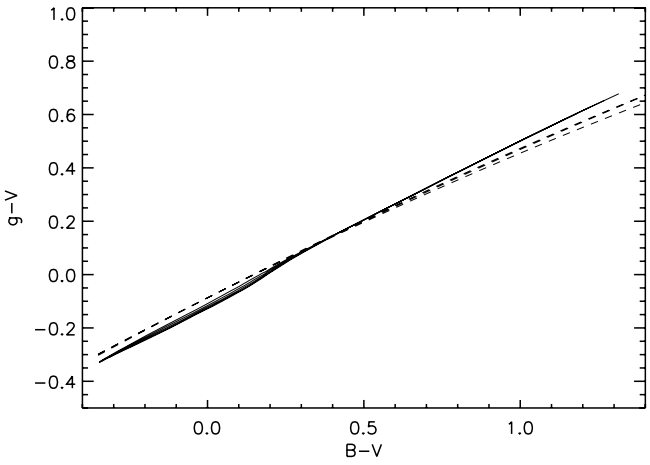

FIG. 7.—Empirical linear color-color relation (*dashed lines*) between the Johnson *B* and *V* and SDSS *u* bands from Rodgers et al. (2006) and the same relation for DA white dwarfs derived from our grid of synthetic photometry (*solid lines*). The various solid lines correspond to gravities ranging from $\log g = 7.0$ to 9.0.

[8] See http://www.sdss.org/dr4/algorithms/sdssUBVRITransform.html#Rodgers2005.

with the observed results for 175 DA white dwarfs observed in this system. Good agreement is found (except for *u*), and zero-point offsets are determined (Table 15).

There are several ways to view the differential corrections given in Table 15. They could be viewed as corrections necessary to bring synthetic magnitudes (and colors) into agreement with the observed magnitudes. Alternately, they could be regarded as corrections necessary to place observed magnitudes onto the *HST* flux scale. A third way to view these corrections is that they establish a set of self-consistent zero-point fluxes for each band on the *HST* flux scale. Basically, they are a set of simple relations that link the *HST* flux scale, synthetic DA white dwarf fluxes, and observed magnitudes. Strictly speaking, these relations apply only to DA white dwarfs and the particular filter sets discussed here. Following procedures similar to those described in this paper, similar (and hopefully not too different) relations can be developed for other blue stars such as DB (helium-rich) white dwarfs, hot subdwarfs, and O, B, and A stars, as well as other filter sets. Much, however, will depend on the fidelity of the stellar models and the filter functions.

Large optical and near-IR surveys are now, or will shortly be, routinely producing large amounts of deep, homogeneous, high-quality photometric data of wide areas of the sky. These surveys include established programs such as 2MASS and SDSS, as well as imminent programs such as the UKIRT Infrared Deep Sky Survey, Pan-STARRS, and the Southern Sky Survey and future programs like the Large Synoptic Survey Telescope survey. It will therefore be possible to calibrate high-fidelity multiband-pass databases on enormous numbers of stellar, as well as nonstellar, objects. For well-defined classes of stars, accurate synthetic photometry can complement such observations to photometrically identify various targets, as well as to extract photometric effective temperatures, gravities, etc. Interstellar reddening is also a potential problem for more distant objects; however, there is no reason that standard reddening-correction techniques cannot be applied.

We wish to thank. Steven Kent and Douglas L. Tucker for providing access to unpublished SDSS magnitudes for GD 71, GD 153, and G191-B2B and Arlo Landolt for unpublished *UBVRI* fluxes. We also wish to acknowledge Jesus Maíz Apellíniz for useful discussions of his investigations of the synthetic photometry of main-sequence stars; Ralph Bohlin for his advice and assistance regarding the *HST* calibration standards and for the helpful referee's report that he provided; and. S. Kent, D. L. Tucker, and Daniel Eisenstein for useful discussions concerning the calibration of the SDSS data. J. H. acknowledges partial support from NSF grant AST 05-07797. P. B. is a Cottrell Scholar of Research Corporation. This work was also supported in part by the NSERC Canada and by the Fonds Québecois de la Recherche sur la Nature et les Technologies Québec.

This publication makes use of data products from the Two Micron All Sky Survey, which is a joint project of the University of Massachusetts and the Infrared Processing and Analysis Center, California Institute of Technology, funded by the National Aeronautics and Space Administration and the National Science Foundation.

Funding for the creation and distribution of the SDSS Archive has been provided by the Alfred P. Sloan Foundation, the Participating Institutions, the National Aeronautics and Space Administration, the National Science Foundation, the US Department of Energy, the Japanese Monbukagakusho, and the Max Planck Society. The SDSS Web site is at http://www.sdss.org. The SDSS is managed by the Astrophysical Research Consortium for the Participating Institutions. The Participating Institutions are the University of Chicago, Fermilab, the Institute for Advanced Study, the Japan Participation Group, The Johns Hopkins University, the Korean Scientist Group, Los Alamos National Laboratory, the Max Planck Institute for Astronomy, the Max Planck Institute for Astrophysics , New Mexico State University, the University of Pittsburgh, the University of Portsmouth, Princeton University, the US Naval Observatory, and the University of Washington.

REFERENCES

Allen, C. W. 1973, Astrophysical Quantities (London: Athlone)
Bergeron, P., Ruiz, M. T., & Leggett, S. K. 1997, ApJS, 108, 339
———. 2001, ApJS, 133, 413
Bergeron, P., Saffer, R. A., & Liebert, J. 1992, ApJ, 394, 228
Bergeron, P., Wesemael, F., & Beauchamp, A. 1995, PASP, 107, 1047 (BWB95)
Bessell, M. S. 1990, PASP, 102, 1181
Bessell, M. S., & Brett, J. M. 1988, PASP, 100, 1134
Bessell, M. S., Castelli, F., & Plez, B. 1998, A&A, 333, 231 (BCP98)
Bessell, M. S., & Wickramasinghe, D. T. 1978, MNRAS, 182, 275
Bohlin, R. C. 2000, AJ, 120, 437
Bohlin, R. C., Colina, L., & Finley, D. S. 1995, AJ, 110, 1316
Bohlin, R. C., Dickinson, M. E., & Calzetti, D. 2001, AJ, 122, 2118
Bohlin, R. C., & Gilliland, R. L. 2004, AJ, 127, 3508 (BG04)
Castelli, F., & Kurucz, R. L. 1994, A&A, 281, 817
Cohen, M. 1993, AJ, 105, 1860
Cohen, M., Megeath, S. T., Hammersley, P. L., Martin-Luis, F., & Stauffer, J. 2003a, AJ, 125, 2645
Cohen, M., Wheaton, W. A., & Megeath, S. T. 2003b, AJ, 126, 1090
Fitzpatrick, E. L., & Massa, D. 2005, AJ, 129, 1642
Fontaine, G., Brassard, P., & Bergeron, P. 2001, PASP, 113, 409
Fukugita, M., et al. 1996, AJ, 111, 1748
Graham, J. 1972, AJ, 77, 144
Gray, R. O. 1998, AJ, 116, 482
Green, R. F. 1977, Ph.D. thesis, Caltech
Green, R. F., Schmidt, M., & Leibert, J. 1986, ApJS, 61, 305
Hauck, B., & Mermilliod, M. 1998, A&AS, 129, 431
Hayes, D. S. 1985, in IAU Symp. 111, Calibration of Fundamental Stellar Quantities, ed. D. S. Hayes, L. S. Pasinetti, & A. G. D. Philip (Dordrecht: Reidel), 225
Holberg, J. B. 1982, ApJ, 257, 656
Holberg, J. B., & Margargal, K. 2005, in ASP Conf. Ser. 334, 14th European Workshop on White Dwarfs, ed. D. Koester & S. Moehler (San Francisco: ASP), 419
Holberg, J. B., et al. 1991, ApJ, 375, 716
Kawka, A., Vennes, S., Koch, R., & Williams, A. 2002, AJ, 124, 2853
Kodaira, K. 1975, in Problems in Stellar Atmospheres and Envelopes, ed. B. Baschek, W. H. Kegal, & G. Travening (Berlin: Springer), 149
Koester, D., & Weidemann, V. 1982, A&A, 108, 406
Lacombe, P., & Fontaine, G. 1981, A&AS, 43, 367
Landolt, A. U. 1992a, AJ, 104, 340
———. 1992b, AJ, 104, 372
Liebert, J., Bergeron, P., & Holberg, J. B. 2005, ApJS, 156, 47
Maíz Apellániz, J. 2005, AJ, 131, 1184 (MA05)
McCook, G., & Sion, E. M. 1999, ApJS, 121, 1
Mégessier, C. 1995, A&A, 296, 771
Oke, J. B., & Gunn, J. E. 1983, ApJ, 266, 713
Olsen, E. C. 1974, PASP, 86, 80
Oswalt, T. D., Smith, J. A., Wood, M. A., & Hintzen, P. 1996, Nature, 382, 692
Rodgers, C. T., Canterna, R., Smith, J. A., Pierce, M. J., & Tucker, D. L. 2006, AJ, 132, 989
Van Altena, W. F., Lee, T. J., & Hoffleit, E. D. 1994, General Catalog of Trigonometric Parallaxes (New Haven: Yale Univ. Obs.)
Wegner, G. 1979, AJ, 84, 1384
Wegner, G. 1983, AJ, 88, 109
Wood, M. A. 1995, in White Dwarfs, ed. D. Koester & K. Werner (Berlin: Springer), 41
York, D. G., et al. 2000, AJ, 120, 1579